Dry Adhesive Microstructures for Material Handling of Additively Manufactured and Deep Rolled Metal Surfaces with Reference to Mars

Nicole Mensching , Mirja Louisa Krüger , Askar Kvaratskheliya , Daniel Meyer * , Kirsten Tracht , Ilya V. Okulov , Lutz Mädler

Posted Date: 28 April 2023

doi: 10.20944/preprints202304.1169.v1

Keywords: surface properties; dry-adhesive microstructures; deep rolling; additive manufacturing

Article

Dry Adhesive Microstructures for Material Handling of Additively Manufactured and Deep Rolled Metal Surfaces with Reference to Mars

Nicole Mensching [1,2], Mirja Louisa Krüger [1,3], Askar Kvaratskheliya [1,2], Daniel Meyer [1,2,*], Kirsten Tracht [1,3], Ilya Okulov [1,2] and Lutz Mädler [1,2,4]

[1] University of Bremen and MAPEX Center for Materials and Processes, Bibliothekstr. 1, 28359 Bremen, Germany, mensching@iwt-bremen.de (N. M.), krueger@bime.de (M. K.), askar@iwt.uni-bremen.de (A. K.), tracht@bime.de (K. T.), i.okulov@iwt.uni-bremen.de (I. O.), lmaedler@iwt.uni-bremen.de (L.M.)
[2] Leibniz Institute for Materials Engineering IWT, Badgasteiner Straße 3, 28359 Bremen, Germany
[3] Bremen Institute for Mechanical Engineering (bime), University of Bremen, Badgasteiner Str. 1, 28359 Bremen, Germany
[4] University of Bremen, Faculty of Production Engineering, Badgasteiner Straße 2, 28359 Bremen, Germany
* Correspondence: dmeyer@iwt.uni-bremen.de (D. M.), Tel.: +49 421 218 51149

Abstract: Once on Mars, maintenance and repair will be crucial for humans as supply chains including Earth andMars will be very complex. Consequently, the raw material available on mars must be processed and used. Factors such as the energy available for material production play just as important a role as the quality of the material that can be produced and the quality of its surface. With the aim of developing and technically implementing a process chain that meets the challenge of producing spare parts from oxygen-reduced Mars regolith, this paper addresses the issue of low-energy handling. Expected statistically distributed high roughnesses of sintered regolith analogs are approximated in this work by parameter variation in the PBF-LB/M process. For low-energy handling, a dry-adhesive microstructure is used. Investigations are carried out to determine the extent to which the rough surface resulting from the manufacturing process can be smoothed by deep rolling in such a way that the microstructure adheres and enables samples to be transported. For the investigated AlSi10Mg samples (12 mm x 12 mm x 10 mm), the surface roughness varies in a wide range from Sa 7.7 µm to Sa 64 µm after the additive manufacturing process, pull-off stresses of up to 6.99 N/cm² could be realized after deep rolling. This represents an increase in pull-off stresses by a factor of 392.94 compared to the pull-off stresses before deep rolling, enabling handling of even larger specimens. It is noteworthy that specimens with roughness values that were previously difficult to handle can be treated post-deep rolling, indicating a potential influence of additional variables that describe roughness or ripples and are associated with the adhesion effect of the microstructure of the dry adhesive.

Keywords: surface properties; dry-adhesive microstructures; deep rolling; additive manufacturing

1. Introduction

Since new products have to meet high requirements regarding performance and lifetime, innovations are always based on the use of materials as pure as possible. Therefore, making things “as good as possible” instead of as “good as necessary” is the driver of current developments. However, the resources available on earth are limited, and with them the possibilities to continue striving for the optimum in material purity in the future. Thus, recycling is becoming increasingly important, although this may involve restrictions with regard to the material's performance. The degree of required material purity may vary depending on the specific application [2,3].

The underlying motivation for the investigations presented here is therefore to use available raw materials in a way that is appropriate to the application and requirements and to design the workpiece "good enough to use" instead of aiming for unnecessarily high purity levels and lifetimes.

The limited availability of pure resources and the need to produce usable, application-oriented components with the available resources links Earth and Mars with each other. Assuming future

settlement on Mars, maintenance and repair will be crucial for humans as supply chains involving Earth and Mars will be very complex. The available resources in terms of raw material and energy must be sufficient to make things work. The question therefore arises to what extent the regolith available on Mars (among other contents consisting of various oxide compounds such as SiO_2, MgO, Al_2O_3, FeO, CaO) [4] can be used for the generation of components. The optimal proportion of pure materials required for synthesis and the maximum acceptable level of impurities, such as regolith, in a material mixture to ensure sufficient quality for producing construction or spare parts remains unclear. It is important to develop energy-efficient and application-focused production methods for these parts. The results of investigations could have potential implications for the development of materials and products on Earth.

These questions are approached with means of a process chain currently under development (see Figure 1), whose core is formed by a sintering and deep rolling as surface treatment process. Prior to this, investigations were conducted on powder mixtures, including different purity levels. However, these investigations will be covered in a different publication as in this study as a commercially available powder mixture is used.. Following the rolling process, the question of handling possible (semi-finished) products arises. Taking into account the low energy available on Mars [5] over the entire process chain, the heat of the sintering process should, in perspective, benefit the rolling process (lower forces required, higher depth effect with warmer samples [6]).The handing should be done using dry-adhesive microstructures, which can adhere to surfaces without additional forces [7].

Since it is already known that the adhesion of dry-adhesive microstructures depends on the surface properties of the object to be handled [8], the following questions concerning the handling are addressed in this work:

- Is handling of samples of high surface roughness, such as those resulting from sintering or additive manufacturing processes, possible without further machining by a rolling process and if, what is the maximum pull-off stress?
- How large is the improvement in adhesion of the dry-adhesive microstructures due to a rolling process?
- When increasing the specimen size, what proportions of the surfaces should be rolled to ensure adhesion for the time required for handling?

Previous research demonstrated the feasibility of metal production using In-Situ Resource Utilisation (ISRU), most commonly in the form of a metal powder produced by an electrochemical reaction [9–11][8–10][7–9][6–8]. Several structural metals that could be derived from Martian soil are under consideration such as Fe, Al, Si, Mg which potentially allow to produce the metal investigated in this work [11–13]. In this study, the PBF-LB/M method is employed to replicate distinct surface roughness characteristics. The rationale for using this method was based on the similarity between the surface roughness parameters of 3D printing and those of conventional sintering methods [14,15].

Since regolith sintering is still a challenge because of the high required temperature for the process, the investigations in this work approach the questions posed by using AlSi10Mg samples of different roughness produced by means of PBF-LB/M [16]. It is assumed that the surface properties are comparable to those of sintered specimens and that the knowledge gained can be transferred to subsequent investigations.

Hydrostatic deep rolling is used as mechanical surface treatment. Investigations by Denkena et al. on cast AlSi10Mg, show a good formability of the surface using a spherical 6.35 mm tool (HG 6 by Ecoroll AG Celle, Germany). With a deep rolling pressure up to 9 MPa, indentation depths of more than 8 µm and indentation widths of more than 800 µm are generated by the tool in single track experiments [17]. It can be assumed that, comparable with the use of other materials, the depth effect of the process increases with increasing rolling pressure [18] or increased work piece temperature [6], so that in addition to influencing the surface, work hardening and residual compressive stresses result [19]. The fact that deep rolling can be used to smoothen the surface of PBF-LB/M has been demonstrated by previous work on 316L [20,21].

Preprints (www.preprints.org) | NOT PEER-REVIEWED | Posted: 28 April 2023 doi:10.20944/preprints202304.1169.v1

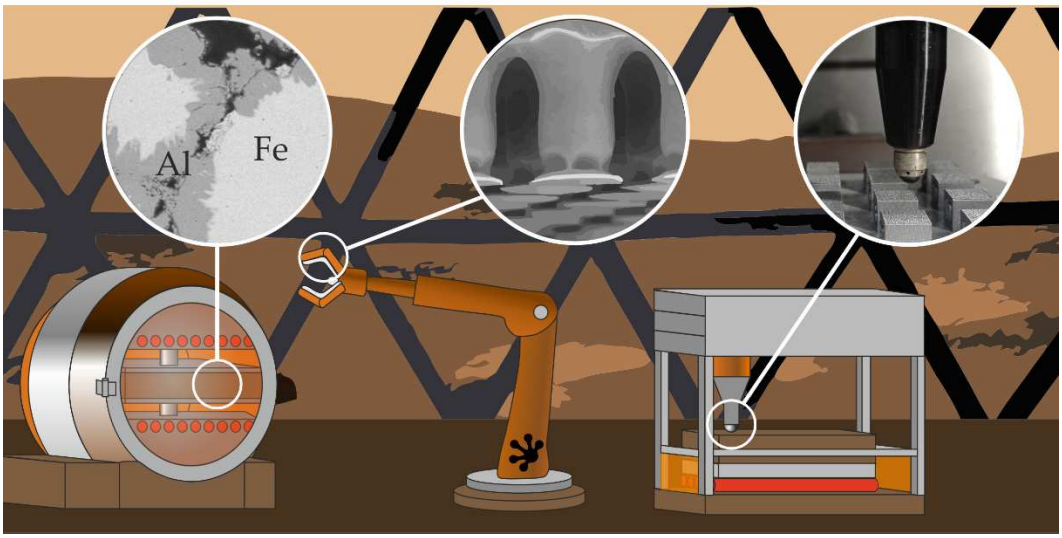

Figure 1. Scheme of the future planned process chain including sintering (left), handling (middle) and strain hardening by deep rolling (right).

The mushroom-shaped microstructure of the dry-adhesive microstructures resembles the microstructure of the leaf beetle foot and not necessarily the microstructure of the gecko foot [22]. Due to the reversible adhesion properties through the Van-der-Waals forces, the dry-adhesive microstructures are used as grippers for various handling processes [7]. This quite new gripper technology works without electricity or compressed air and therefore can be used under a vacuum. When used as a gripper, surface roughness can be an obstacle to adhesion, as the intermolecular interactions occur over a short distance. Excessive roughness can therefore reduce the formation of the interactions [23] and the maximum holding force depending on the object geometry and the material pairing. If the surface roughnesses become too large, the contact is broken and the maximum holding force is reduced. [24]

Gorumlu et al. also found that the microstructures adheres better to smooth surfaces. In their experiments, the dry-adhesive microstructures adheres with an adhesive force of 10 N/cm² on a smooth surface and with an adhesive force of 1 N/cm² on a rough surface with a quadratic mean Rq from 373 nm to 618 nm. [8]

Bauer et al. also conducted investigations with the dry-adhesive microstructures. In the experiments, the dry-adhesive microstructures are pressed onto a flat, rough aluminium specimen. The adhesion in these experiments is 35% to 50% lower compared to experiments on a flat, smooth glass substrate. [25]

In addition, it is clear that the adhesion of the dry-adhesive microstructures is limited by the onset of buckling. Bauer et al. also found that the dry-adhesive microstructures adhere better and have higher pull-off stresses on wavy, rough surfaces than on flat tip structures. [25]

2. Materials and Methods

2.1. Additive manufacturing of samples using laser powder bed fusion (PBF-LB/M)

Spherical gas atomized AlSi10Mg powder supplied by the company Tekna is used for LPBF in this study. The AlSi10Mg powder particles have an average diameter of 45 ± 10 µm. Their chemical composition can be found in Table 1.

Table 1. Initial chemical composition of the powder [26]

Al	*Si*	*Mg*	*Fe*	*Ti*	*Mn*	*Zn*	*others*
85,00 – 87,00 %	9.00 – 11.00 %	0.20 – 0.45 %	≤ 0.50 %	≤ 0.15 %	0.40 %	≤ 0.10 %	0.80 – 1.50 %

Preprints (www.preprints.org) | NOT PEER-REVIEWED | Posted: 28 April 2023 doi:10.20944/preprints202304.1169.v1

The sample generation samples in the form of parallelepipeds (12 x 12 x 10 mm), are additivly manufactured by a PBF-LB/M process (SLM-125HL, by SLM Solutions, Lübeck, Germany). The samples consist of two parts, namely substrate (lower part) and finishing (higher part). Both parts are fabricated using the laser beam diameter of ~ 70 µm and the powder layer thickness of 30 µm. The substrate part is manufactured using a laserpower of 300 W, a hatch distance of 150 µm and a scan speed of 1000 mm/s. In Figure 2 visualisati of realised strategy could be found

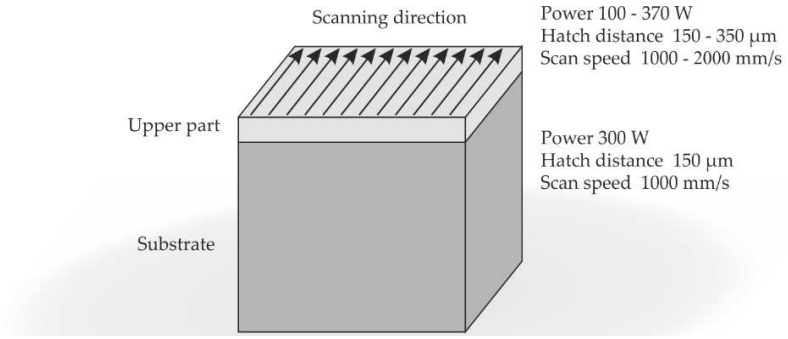

Figure 2. Visualisation of the strategy applied when printing and using parameters.

In order to obtain different mean arithmetic height Sa parameters, the finishing part (last three layers) are manufactured using different laser parameters (Table 3). Specifically, the laser power is varied from 100 W to 370 W. The hatch distance is varied from 150 µm to 350 µm and the scan speed is varied from 1000 mm/s to 2000 mm/s. The additive manufacturing process is carried out under high-purity argon atmosphere . The variation of the previously mentioned parameters are chosen following Maamoun, Xue et al., as they reached surface roughness between 5 µm and 14 µm[27].

2.2. Characterisation of the surface

After the production of the samples using the PBF-LB/M process, the surfaces of the 24 samples, are examined with a 3D laser-scanning microscope using a 5x magnification (VK-X100K/X200K 3D laser-scanning microscope by Keyence Deutschland GmbH, Neu-Isenburg, Germany). The surface quality is determined according to DIN EN ISO 25178 with the analysis software "VK Analyse Modul". The mean arithmetic height Sa is determined for all samples by evaluating the entire area of the microscope image using the mentioned ISO-standard. Subsequently, 12 of the 24 samples are deep rolled and then the mean arithmetic heights are determined again. To decide which samples are to be deep rolled, the different surface parameters mean arithmetic height Sa, maximum height Sz and total height of the ripple Wz are compared between the specimen and matching pairs are formed, one sample of each pair was deep rolled (cf. Table 3).

2.3. Deep rolling

Deep rolling of the PBF-LB/M samples are performed on a 3-axis CNC machining center (DMC 65V by Deckel Maho, Pfronten, Germany). The experimental setup can be seen in Figure 3 (a). A hydrostatic deep rolling tool with a spherical ceramic tip HG 6 (diameter d_b = 6.3 mm) produced by Ecoroll (Ecoroll AG Werkzeugtechnik, Celle, Germany) is utilized to generate a deep rolled area of 10 mm x 10 mm. Due to the contact width of the deep rolling tool and the process design focusing on the center of the tool the actual deep rolled area of the specimens is slightly larger. Therefore, an area of 10 mm x 10 mm can be selected to test the dry-adhesive microstructure tapes without effects of the non-deep rolled outer area. The deep rolling direction is chosen perpendicular to the visible PBF-LB/M surface structure. Using a step over of 0.1 mm each area is generated by 100 single deep rolling tracks. Figure 3 (b) shows a sample before and Figure 3 (c) a sample after deep rolling. In Figure 3 (c), the 10 mm x 10 mm area generated during the process can be seen marked red. In addition, it is visible that the actual deep rolled area is larger by the indentation width of the deep rolling tool.

Preprints (www.preprints.org) | NOT PEER-REVIEWED | Posted: 28 April 2023 doi:10.20944/preprints202304.1169.v1

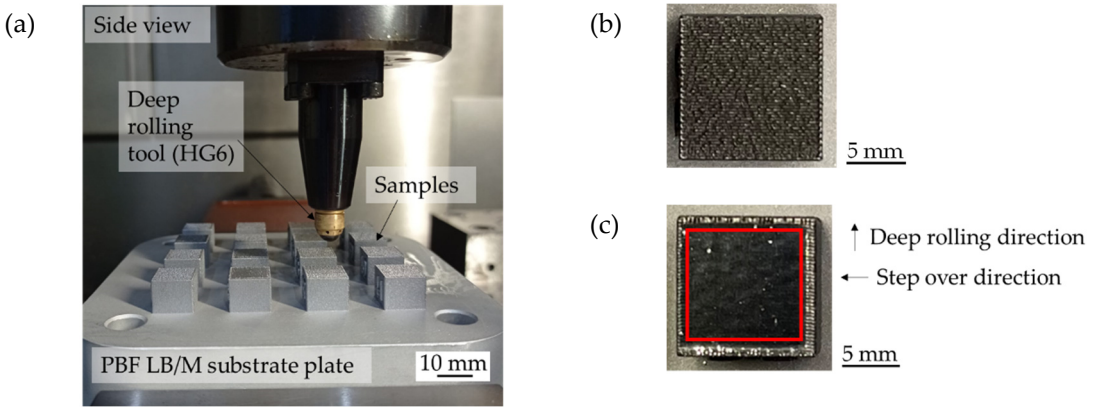

Figure 3. Experimental setup (a); sample before (b) and after deep rolling an area of 10 mm x 10 mm (c).

The force measurement during the deep rolling process is performed with a piezoelectric 3-component dynamometer (Typ 9257 B, Kistler Instrumente GmbH, Sindelfingen, Germany) equipped by a Kistler charge amplifier Typ 5019 A. The deep rolling pressure of 10 MPa, selected in accordance with Denkena et al. [17], resulted in a deep rolling force F_r of 242.33 N ± 5.97 N. The process parameters and force measurement settings are summarized in Table 2. After deep rolling the specimen are electrolytically cut off the aluminum base plate for further investigations.

Table 2. Deep rolling parameter and force measurement settings.

Parameter	*Value*
tool diameter d_b	6.35 mm
deep rolling pressure p_{dr}	10 MPa
deep rolling force F_r	242.33 N ± 5.97 N
step over so	0.1 mm
rolling speed v_r	100 mm/min
lubricant	8%-emulsion
size of deep rolled area f_a	10 × 10 mm2
low pass filter Lp	300 Hz
sampling rate sr	1 kHz

2.4. Method for quantifying adhesion

The samples are cleaned in an ultrasonic bath (Bandelin Sonorex TK 52 by Bandelin electronic GmbH & Co. Kg, Berlin, Germany) with isopropanol for 15 minutes and then dried with compressed air so that they are free of dust and grease. An ElectroPuls® E1000 testing machine (by Instron GmbH, Darmstadt, Germany) is used to determine the pull-off stress $\sigma_{pullmax}$. The machine is equipped with the load cell Dynacell - Dynamic Load Cell ±250 N (±56 lbf) (Instron GmbH, Darmstadt, Germany). The specimens and the dry-adhesive microstructures are attached to specially manufactured adapters and then clamped in the chucks of the testing machine. The testing machine and the clamped adapters with a sample and the dry-adhesive microstructure respectively can be seen in Figure 4 (a) and (b).

Preprints (www.preprints.org) | NOT PEER-REVIEWED | Posted: 28 April 2023 doi:10.20944/preprints202304.1169.v1

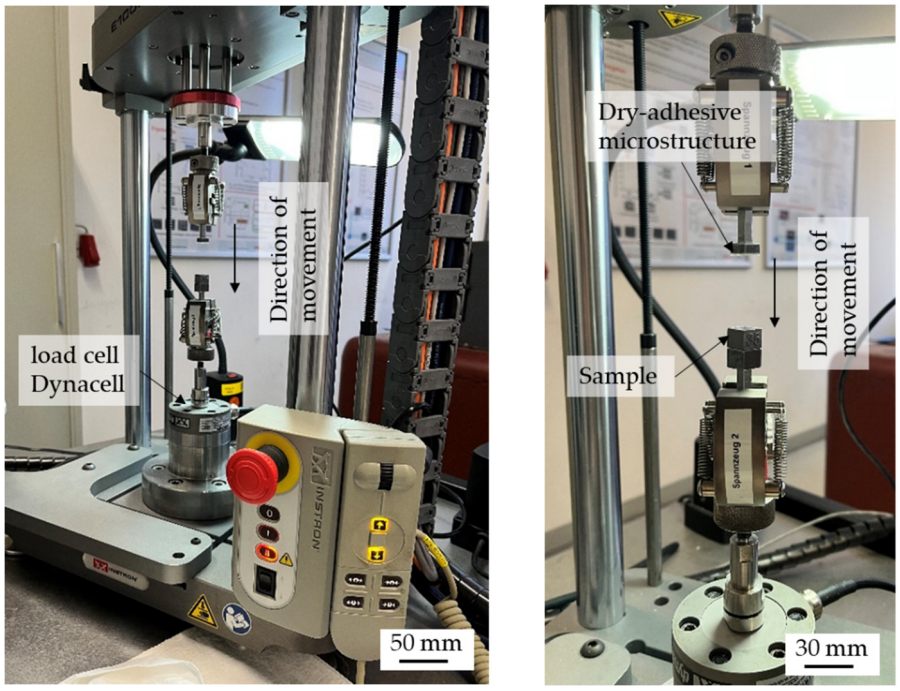

(a) (b)

Figure 4. ElectroPuls® E1000 testing machine (a) with the clamped adapters and the attached specimens or dry-adhesive microstructures (b).

As dry-adhesive microstructure tape Gecko® Nanoplast® (Klettband Technik, Waldenbuch, Germany) is used for the experiments. This tape has a mushroom-shaped surface, whereby the adhesion between the samples and the dry-adhesive microstructures is realised by Van der Waals forces. The size of the dry-adhesive microstructure tape in each experiment is 10 mm x 10 mm. The sections of the tape are cut out with the help of a shaping punch.

A machining program is developed to determine the pull-off stress. The program moves the upper chuck down at a speed of 0.1 mm/s until the dry-adhesive microstructures touches the sample. Then the contact pressure is increased by 2 N/s until a contact pressure of 10 N is reached. This pressure is maintained for 10 s before the upper collet with the dry-adhesive microstructures is raised again at a speed of 0.1 mm/s and the pull-off stress can be measured.

For statistical validation, the pull-off stress is determined five times for each sample. A new dry-adhesive microstructure is used for each new adhesion and peel-off test in order to exclude defects due to wear or contamination. After each adhesion test, the PBF-LB/M samples are cleaned with ethanol to remove dirt or torn microstructures.

3. Results

3.1. Surface roughness before and after deep rolling

The surface of the PBF-LB/M samples is characterized using the 3D laser-scanning microscope (VK-X100K/X200K 3D laser scanning microscope by Keyence, Deutschland GmbH, Neu-Isenburg, Germany) before and after deep rolling. The images are evaluated according to DIN EN ISO 25178. The Sa values determined for the individual samples are shown in Table 3. It can be seen that the roughness's of the samples are significantly reduced by the rolling process. Before deep rolling, the maximum Sa value is 64 µm and the minimum Sa value 7.7 µm. After deep rolling, the maximum Sa value is 19.1 µm and the minimum Sa value is 0.3 µm. The mean arithmetic height Sa values after sample generation and deep rolling can be compared with the results of Wielki and Meyer [20,21].

Preprints (www.preprints.org) | NOT PEER-REVIEWED | Posted: 28 April 2023 doi:10.20944/preprints202304.1169.v1

Table 3. Mean arithmetic height of the 24 samples.

Sample no.	*laser power P, hatch distance D_h, scan speed V_s*	*mean arithmetic height Sa before deep rolling*	*mean arithmetic height Sa after deep rolling*	*Roughness reduction ΔSa*
1	100 W, 250 µm, 1500 mm/s	9.8 µm	0.3 µm	97 %
2	100 W, 350 µm, 1500 mm/s	10.3 µm		
3	100 W, 350 µm, 2000 mm/s	7.7 µm	0.6 µm	92 %
4	370 W, 350 µm, 1000 mm/s	13.3 µm		
5	370 W, 350 µm, 1500 mm/s	50.8 µm	1.2 µm	98 %
6	370 W, 350 µm, 2000 mm/s	54.8 µm		
7	200 W, 250 µm, 1500 mm/s	57.3 µm	5.5 µm	90 %
8	100 W, 250 µm, 2000 mm/s	8.7 µm		
9	200 W, 350 µm, 1500 mm/s	17.8 µm	6.0 µm	66 %
10	100 W, 150 µm, 1500 mm/s	27.0 µm		
11	200 W, 250 µm, 2000 mm/s	31.6 µm	6.2 µm	80 %
12	200 W, 250 µm, 1000 mm/s	31.2 µm		
13	300 W, 250 µm, 1000 mm/s	20.5 µm	6.8 µm	67 %
14	200 W, 350 µm, 2000 mm/s	37.0 µm		
15	200 W, 350 µm, 1000 mm/s	23.5 µm	6.8 µm	71 %
16	100 W, 350 µm, 1000 mm/s	27.5 µm		
17	300 W, 350 µm, 1000 mm/s	60.6 µm	6.8 µm	89 %
18	100 W, 350 µm, 1500 mm/s	10.4 µm		
19	100 W, 250 µm, 1000 mm/s	64.0 µm	7.7 µm	88 %
20	100 W, 350 µm, 1000 mm/s	50.3 µm		
21	300 W, 250 µm, 1500 mm/s	23.8 µm	10.9 µm	54 %
22	300 W, 350 µm, 1500 mm/s	22.7 µm		
23	200 W, 350 µm, 1000 mm/s	32.0 µm	15.3 µm	52 %
24	200 W, 250 µm, 2000 mm/s	37.0 µm		

Depending on the surface roughness after the sample generation, the deep rolling process was able to reduce the Sa-values up to 98 % (e.g. sample 5). Regarding the considered range of surface roughness's, the potential for smoothing is higher with a higher initial roughness. Figure 5 exemplarily shows the surface topography of sample no. 19 before (Sa = 64.0 µm) and after deep rolling (Sa = 7.7 µm). The results show that deep rolling leads to a reduction in surface profile elevations, which is frequently observed after the specimen generation. Furthermore, a decrease in roughness over the entire surface area is observed following the rolling process. Reducing the roughness level allows more individual microstructures of the dry adhesive tape to adhere to the surface and increases the maximum pull-off stress.

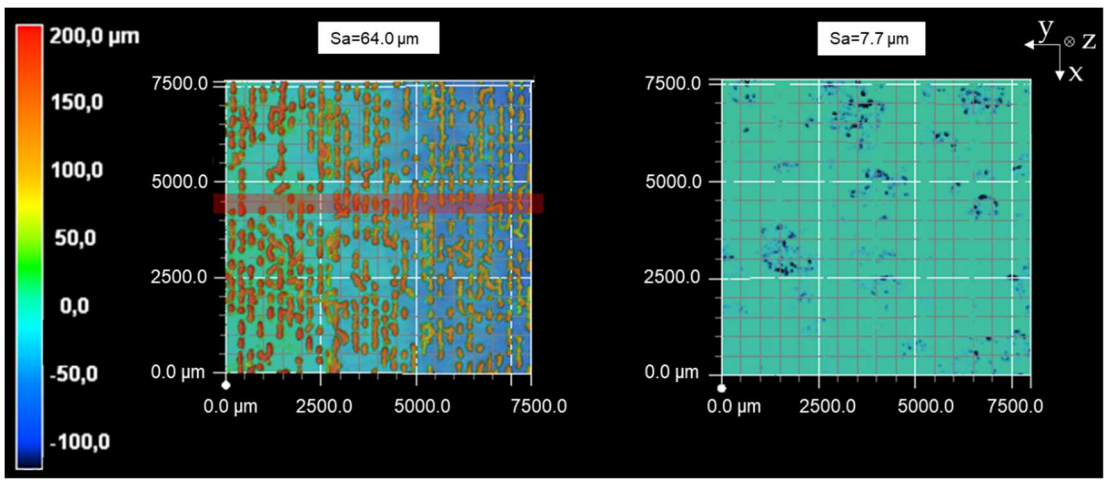

Preprints (www.preprints.org) | NOT PEER-REVIEWED | Posted: 28 April 2023 doi:10.20944/preprints202304.1169.v1

Figure 5. Surface topography before (left) and after (right) deep rolling sample 19.

Figure 6 shows an example of the normal forces determined during deep rolling. Shown in orange is the curve associated with specimen 19. The average values are around 242 N (cf. section 2.4) and the curve shows an up and down of the force depending on the topography elevations traversed. The deep rolled track on which the force measurement is based, is indicated on the left side of Figure 5 as a red area. For comparison, the force measurement of a significantly smoother specimen (Sa = 9.8 µm, sample 1) is shown in comparison on the secondary axis in Figure 6. In average, the deep rolling force are comparable in both cases, but the black curve shows a more constant forces level, because fewer topographic elevations had to be flattened.

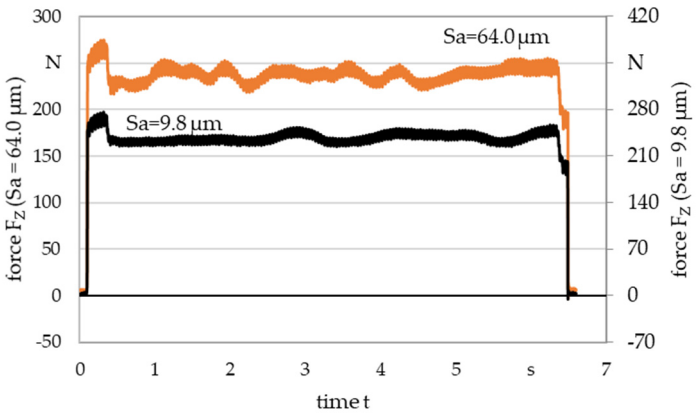

Figure 6. Deep rolling force determined exemplarily while smoothening different surface roughness.

3.2. Adhesion before and after deep rolling

After evaluating the microscope images, the experiments described in section 2.3 are carried out and an average value of the pull-off stress is determined for each sample. The pull-off stress for the samples before and after deep rolling is shown in Figure 7. The Sa values of the samples are plotted in µm and the corresponding pull-off stress in N/cm². The maximum pull-off stress for the PBF-LB/M printed samples (blue) is 0.12 N/cm² and the minimum pull-off stress is 0.01 N/cm². In addition, the pairs of samples that belong together are arranged next to each other. In Figure 7, the maximum pull-off stress for the PBF-LB/M printed and deep rolled samples (green) is 7 N/cm² and the minimum pull-off stress is 2.2 N/cm².

Preprints (www.preprints.org) | NOT PEER-REVIEWED | Posted: 28 April 2023 doi:10.20944/preprints202304.1169.v1

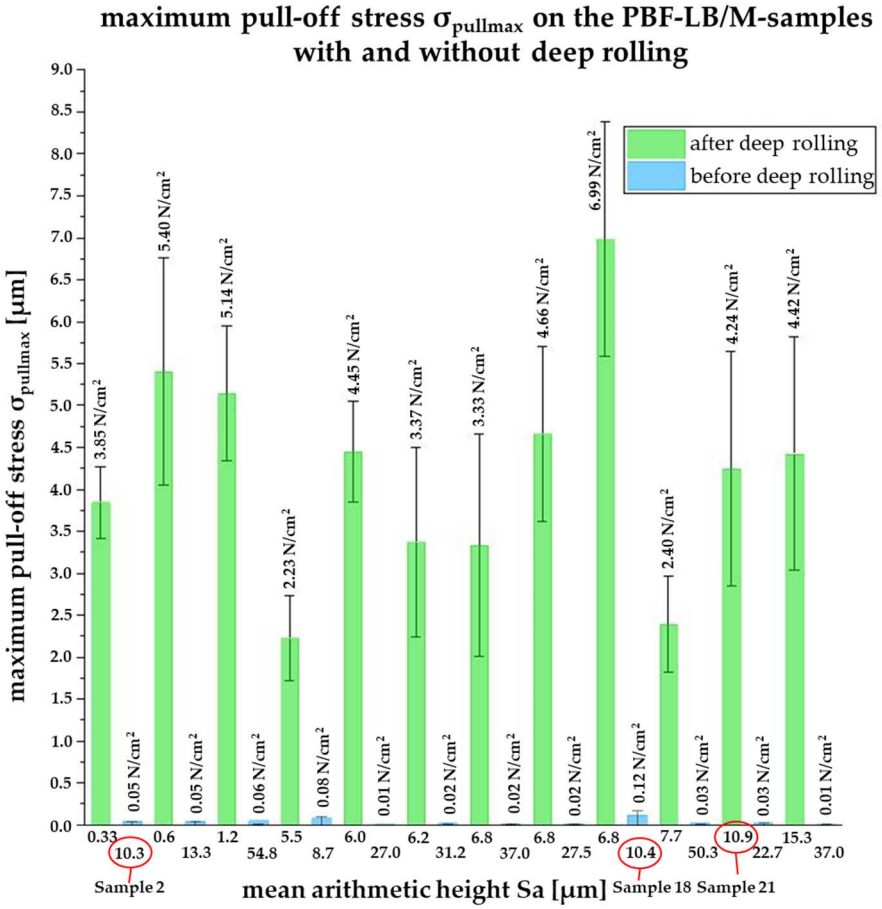

Figure 7. Maximum pull-off stress $\sigma_{pullmax}$ on the PBF-LB/M-samples with (green) and without deep rolling (blue). The matching pairs from Table 3 are arranged next to each other.

4. Discussion

While the pull-off stress directly after the specimen generation (Sa values between 7.7 µm and 64 µm) is less than 0.2 N/cm², pull-off stresses of up to 6.99 N/cm² are resulting after deep rolling. Accordingly, the pull-off stress is up to 35 times higher on the PBF-LB/M-samples after deep rolling than on the non-post-processed samples. This is because of the smoothing of the surface by deep rolling which allows more individual microstructures of the adhesive tape to adhere to the surface and therefore increase the maximum pull-off stress [24]. This can be seen in Figure 8. There, a deep rolled and a non deep rolled surface topography are schematically shown opposite the dry adhesive microstructures.

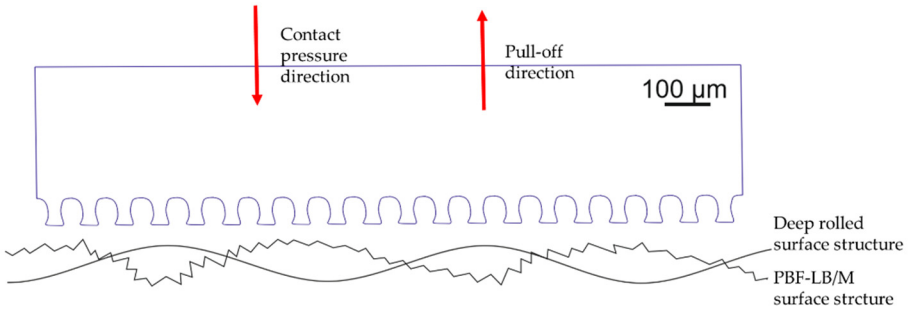

Figure 8. Schematic representation of the dry-adhesive microstructures versus a non-reworked surface topography and deep rolled surface topography.

Preprints (www.preprints.org) | NOT PEER-REVIEWED | Posted: 28 April 2023 doi:10.20944/preprints202304.1169.v1

For a further discussion, the samples where the Sa values before and after deep rolling are of the same order of magnitude, but have resulted in significantly different pull-off stresses, are of particular interest. Therefore, Table 4 compares results obtained on selected samples. While before deep rolling Sa values of 10.3 and 10.4 µm resulted in pull-off stresses of 0.05 and 0.12 N/cm², respectively, while a slightly higher Sa value after deep rolling of about 10.9 µm resulted in a pull-off stress of 4.24 N/cm². The surface topographies from samples 2, 18, and 21 are shown in Figure 9. Samples 2 and 18 are not post-processed and sample 21 is post-processed by deep rolling. Based on the surface structures, the smoothing of the surface by deep rolling becomes clear. As a result, more dry-adhesive microstructures were able to form a contact with the specimen surface.

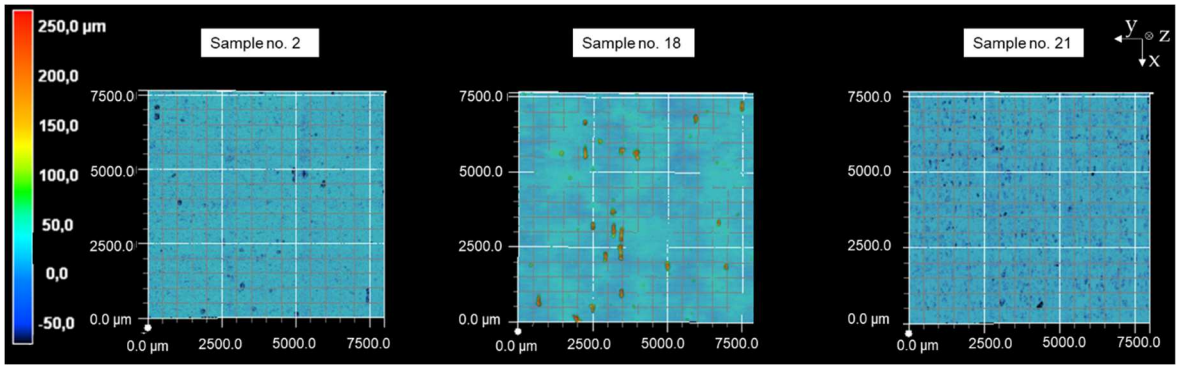

Figure 9. Surface topographies of samples 2, 18 and 21.

Considering only the Sa value alone to assess the smoothing potential of deep rolling allows an initial assessment, however, other quantities should be considered for future prediction of the adhesion of dry-adhesive microstructures. As shown in Table 4, the samples differ in their height of the core area Sk, their material fraction Smr1, as well as their material fraction Smr2 values. With the help of these parameters, the Abbott-Firestone curve, which is shown schematically in Figure 10, can be determined for the individual samples. The Abbott-Firestone curve is a graphical plot of the material ratio against the height of the profile. The material ratio describes the density of the material at the respective height. The flatter the Abbott-Firestone curve, the higher the material density in the sample surface, which means that more dry-adhesive microstructures can form contact with the surface..

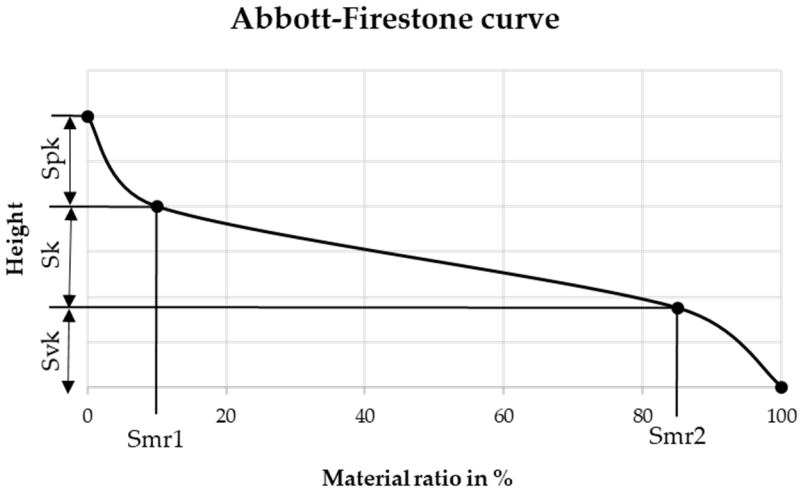

Figure 10. Schematic Abbott-Firestone curve.

The schematic diagram shows the reduced peak height Spk, the core height Sk, the reduced valley depth Svk, the peak material portion Smr1 and the valley material portion Smr2. With the help of these surface parameters, the Abott-Firestone curve can be generated for each sample.

Preprints (www.preprints.org) | NOT PEER-REVIEWED | Posted: 28 April 2023 doi:10.20944/preprints202304.1169.v1

The Abbott-Firestone curves for samples 2, 18 and 21 are shown in Figure 11 and the Abbott-Firestone curves for all samples are shown in Figure 12.

These quantities, taken from bearing area curves (also known as Abbott-Firestone curves), indicate a much flatter curve shape after deep rolling compared to the PBF-LB/M samples, due to the lower core height and measured material fractions.

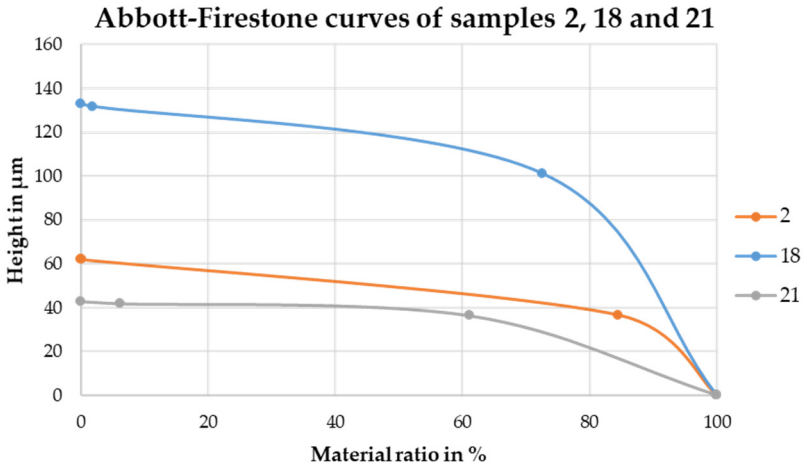

Figure 11. Abbott-Firestone curves of samples 2, 18 and 21.

Thus, the course of the bearing area curve i.e. the shape of the surface topography has an influence on the adhesion of the dry-adhesive microstructures. The curve of sample 21 is significantly flatter than the curves of the samples that were not post-processed. This suggests that the material density in the sample surface is higher, which allows more individual microstructures to adhere to the surface, increasing the maximum pull-off stress [24].

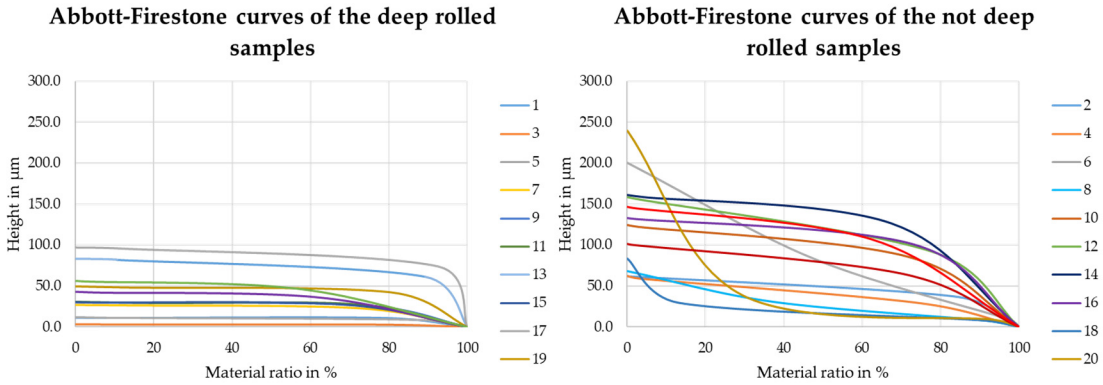

Figure 12. Abbott-Firestone curves of all samples.

This observation is confirmed by the Abbott-Firestone curves of the further samples. The curves of the deep rolled samples are clearly flatter and have a lower starting height compared to the Abbott-Firestone curves of the non deep rolled samples.

Table 4. Samples with comparable Sa-values (gray background: deep rolled specimen).

Sample no.	2	18	21
Mean arithmetic height Sa	10.3 µm	10.4 µm	10.9 µm
Pull-off stress $\sigma_{pullmax}$	0.05 N/cm²	0.12 N/cm²	4.24 N/cm²
Height of the core area Sk	25.32 µm	30.64 µm	5.50 µm
Material fraction Smr1	0.18 %	1.91 %	6.11 %
Material fraction Smr2	84.53 %	72.61 %	61.08 %

Preprints (www.preprints.org) | NOT PEER-REVIEWED | Posted: 28 April 2023 doi:10.20944/preprints202304.1169.v1

Arithmetic average roughness Ra	10.3 µm	10.4 µm	10.9 µm
Mean roughness depth Rz	367.0 µm	262.5 µm	502.5 µm
Maximum height of the ripple Wz	214.7 µm	203.9 µm	366.3 µm

5. Summary and Outlook

In this work, additively manufactured samples of varied surface roughness made of AlSi10Mg are investigated with regard to the adhesion conditions for dry-adhesive microstructures by means of an adapted tensile test. For this purpose, dry-adhesive microstructures of dimensions 10 mm x 10 mm are pressed onto the specimen surface for 10 s with a contact force of 10 N and the pull-off stress was measured during release. It can be stated that the smoothing of the surface, as a result of an intermediate deep rolling process, leads to an increase in the determined pull-off stress

The mean arithmetic height Sa, which is used to assess the surface quality, allows an initial assessment of the smoothening resulting after deep rolling. The parameters determined in this work allow the questions posed at the beginning to be answered and initial conclusions to be drawn with regard to the perspective processing and handling of sintered samples of larger dimensions made of regolith:

- An adhesion of the used dry-adhesive microstructures on the PBF-LB/M -samples could be determined. The maximum pull-off stress was 0.12 N/cm².
- The determined pull-off stresses show an increase by a factor of 26.41 to 392.94 after deep rolling. Handling based on adhesion of the dry-adhesive microstructure on a deep rolled surface is therefore possible.
- The Abbott-Firestone curves of the deep rolled specimens are much flatter and have a lower starting height compared to the curves of the non deep rolled specimens, allowing more dry adhesive microstructures to form contact with the specimen surface.
- On Mars, dry-adhesive microstructures will be used to handle sintered sheets of regolith with a diameter up to 68 mm and a maximum height of 5 mm. Assuming that the surface roughness and quality is comparable to that of the AlSi10Mg used in this paper, at least 1/8 of the surface must be deep rolled. It is also crucial where the deep-rolled surface is located on the sheet so that no shear forces act on the dry-adhesive microstructures during gripping and handling.

In order to develop a demonstrator within the framework of subsequent work that allows the process chain shown schematically in Figure 1 to be implemented, the following aspects are the focus of further investigations:

a) Generation and processing of sintered specimens

The next stages of the work will investigate samples from artificially contaminated materials to the level of materials obtained electrochemically from regolith, as well as the effect of different compositions and sintering regimes on surface properties. It can be assumed that the material properties of sintered samples made of the material investigated in this work (AlSi10Mg) slightly differ in their surface and subsurface properties from those produced by means of PBF-LM/B. Therefore, investigations on the possible influence of (deep) rolling as well as on the handling by means of the dry-adhesive microstructure have to be carried out systematically in dependence of the sample composition.

b) Systematic study of the adhesion conditions

In order to further understand the adhesion behavior of the dry-adhesive microstructures, experiments with different materials and manufacturing processes of the samples are carried out in the following. In addition, the wear and contamination behavior will be analyzed.

Author Contributions: Conceptualization, methodology, investigation, N.M., M.K., and A.K. writing—original draft preparation, N.M., M.K., and A.K.; writing—review and editing, D.M., L.M., I.O., and K.T.; supervision, D.M., L.M., I.O., and K.T. All authors have read and agreed to the published version of the manuscript.

Funding: The Federal State of Bremen and the University of Bremen support the 'Humans on Mars Initiative' with funding for seven seed projects until the end of 2024. The initiative employs more than 20 early career researchers and supports undergraduate education related to space exploration. https://www.uni-bremen.de/en/aerospace-at-the-univer-sity-of-bremen/humans-on-mars.

Institutional Review Board Statement: Not applicable.

Data Availability Statement: The data presented in this study are available on request from the corresponding author.

Acknowledgments: This project is part of the 'Humans on Mars Initiative' funded by the Federal State of Bremen and the University of Bremen.

Conflicts of Interest: The authors declare no conflict of interest.

References

1. Czotscher, T.; Wielki, N.; Vetter, K.; Vollertsen, F.; Meyer, D. Rapid Material Characterization of Deep-Alloyed Steels by Shock Wave-Based Indentation Technique and Deep Rolling. *Nanomanuf Metrol* **2019**, *2*, 56–64, doi:10.1007/s41871-019-00036-4.
2. Briant, C.L. Impurities in Engineering Materials - Impact, Reliability and Control. *Materials and Manufacturing Processes* **2000**, *15*, 155–156, doi:10.1080/10426910008912979.
3. Lipiński, T.; Ulewicz, R. The effect of the impurities spaces on the quality of structural steel working at variable loads. *Open Engineering* **2021**, *11*, 233–238, doi:10.1515/eng-2021-0024.
4. Economou, E.; Rieder, R.; Wänke, H.; Turkevich, A.; Brueckner, J.; Dreibus, G.; Crisp, J.; McSween, H. The chemical composition of Martian rocks and soil: preliminary analyses. *Lunar and Planetary Science Conference* **1988**.
5. Rucker, M.A. Integrated Surface Power Strategy for Mars **2015**.
6. Schulze, V.; Bleicher, F.; Groche, P.; Guo, Y.B.; Pyun, Y.S. Surface modification by machine hammer peening and burnishing. *CIRP Annals* **2016**, *65*, 809–832, doi:10.1016/j.cirp.2016.05.005.
7. Hensel, R.; Moh, K.; Arzt, E. Engineering Micropatterned Dry Adhesives: From Contact Theory to Handling Applications. *Adv. Funct. Mater.* **2018**, *28*, 1800865, doi:10.1002/adfm.201800865.
8. Gorumlu, S.; Aksak, B. Sticking to rough surfaces using functionally graded bio-inspired microfibres. *R. Soc. Open Sci.* **2017**, *4*, 161105, doi:10.1098/rsos.161105.
9. Haskin, L.A. Oxygen and Iron Production by Electrolytic Smelting of Lunar Soil **1991**.
10. Sibille, L.; Dominguez, J.A. Joule-heated Molten Regolith Electrolysis Reactor Concepts for Oxygen and Metals Production on the Moon and Mars. *International Conference on Environmental Systems (ICES)* **2012**, *42nd*.
11. Curreri, P.A.; Ethridge, E.C.; Hudson, S.B.; Miller, T.Y.; Grugel, R.N.; Sadoway, D.R.; Sen, S. Process Demonstration For Lunar In Situ Resource Utilization— Molten Oxide Electrolysis **2006**.
12. Stefanescu, D.M.; Grugel, R.N.; Curreri, P.A. In Situ Resource Utilization for Processing of Metal Alloys on Lunar and Mars Bases **1998**, 266–274, doi:10.1061/40339(206)32.
13. Shaw, M.; Humbert, M.; Brooks, G.; Rhamdhani, A.; Duffy, A.; Pownceby, M. Mineral Processing and Metal Extraction on the Lunar Surface - Challenges and Opportunities. *Mineral Processing and Extractive Metallurgy Review* **2022**, *43*, 865–891, doi:10.1080/08827508.2021.1969390.
14. Cai, C.; Song, B.; Xue, P.; Wei, Q.; Wu, J.; Li, W.; Shi, Y. Effect of hot isostatic pressing procedure on performance of Ti6Al4V: Surface qualities, microstructure and mechanical properties. *Journal of Alloys and Compounds* **2016**, *686*, 55–63, doi:10.1016/j.jallcom.2016.05.280.
15. Sadali, M.F.; Hassan, M.Z.; Ahmad, F.; Yahaya, H.; Rasid, Z.A. Influence of selective laser melting scanning speed parameter on the surface morphology, surface roughness, and micropores for manufactured Ti6Al4V parts. *J. Mater. Res.* **2020**, *35*, 2025–2035, doi:10.1557/jmr.2020.84.
16. Dou, R.; Tang, W.Z.; Wang, L.; Li, S.; Duan, W.Y.; Lui, M.; Wang, G.). Sintering of lunar regolith structures fabricated via digital light processing. *Ceramics International* **2019**, *45(14)*, 17210–17215.
17. Denkena, B.; Krödel, A.; Heikebrügge, S.; Meyer, K.; Pillkahn, P. Surface topography after deep rolling with milling kinematics. *Prod. Eng. Res. Devel.* **2021**, *15*, 587–593, doi:10.1007/s11740-021-01031-9.
18. Berstein, G.; Fuchsbauer, B. Festwalzen und Schwingfestigkeit. *Mat.-wiss. u. Werkstofftech.* **1982**, *13*, 103–109, doi:10.1002/mawe.19820130309.
19. Schulze, V. *Modern mechanical surface treatment*: *States, stability, effects*. Zugl.: Karlsruhe, Univ., Habil.-Schr., 2004; Wiley-VCH Verl.: Weinheim, 2006, ISBN 3-527-31371-0.
20. Wielki, N.; Meyer, D. Potential of deep rolling as a finishing process directly after SLM to generate beneficial surface and subsurface properties. *euspen' 19th International Conference & Exhibition* **2019**, 370–371.
21. Meyer, D.; Wielki, N. Internal reinforced domains by intermediate deep rolling in additive manufacturing. *CIRP Annals* **2019**, *68*, 579–582, doi:10.1016/j.cirp.2019.04.012.

22. Kizilkan, E.; Gorb, S.N. Bioinspired Further Enhanced Dry Adhesive by the Combined Effect of the Microstructure and Surface Free-Energy Increase. *ACS Appl. Mater. Interfaces* **2018**, *10*, 26752–26758, doi:10.1021/acsami.8b06686.
23. Arzt, E.; Quan, H.; McMeeking, R.M.; Hensel, R. Functional surface microstructures inspired by nature – From adhesion and wetting principles to sustainable new devices. *Progress in Materials Science* **2021**, *120*, 100823, doi:10.1016/j.pmatsci.2021.100823.
24. Meiners, F.; Tuitje, C.; Hogreve, S.; Tracht, K. Model-based prediction of the detachment of microspheres from dry-adhesive gripper surfaces by bending. *Procedia CIRP* **2022**, *115*, 101–106, doi:10.1016/j.procir.2022.10.057.
25. Bauer, C.T.; Kroner, E.; Fleck, N.A.; Arzt, E. Hierarchical macroscopic fibrillar adhesives: in situ study of buckling and adhesion mechanisms on wavy substrates. *Bioinspir. Biomim.* **2015**, *10*, 66002, doi:10.1088/1748-3190/10/6/066002.
26. Tekna Advanced Materials Inc. *TekmatTM AlSi10Mg.45/10-A*: *Data Sheet;* 2895 Industrial Blvd., Sherbrooke, Qc, Canada, J1L 2T9, 2020. Available online: https://www.tekna.com.
27. Maamoun, A.H.; Xue, Y.F.; Elbestawi, M.A.; Veldhuis, S.C. Effect of Selective Laser Melting Process Parameters on the Quality of Al Alloy Parts: Powder Characterization, Density, Surface Roughness, and Dimensional Accuracy. *Materials (Basel)* **2018**, *11*, doi:10.3390/ma11122343.